Disappearance of Curie Temperature of BaTiO$_3$ Nanopowder Synthesised by High Energy Ball Mill

S. Pendse and R. K. Goyal[*]

Department of Metallurgy and Materials Science, College of Engineering, Shivaji Nagar, Pune – 411 005, India.

Abstract

Planetary ball mill was used to synthesize nanopowder from commercial micron sized BaTiO$_3$ powder under dry condition. The ball milling time was varied from 0 to 20 h in steps of 5 h. The synthesized powder was characterized using X-ray diffraction (XRD), BET surface area analyser, scanning electron microscope (SEM) and differential scanning calorimetry (DSC). XRD showed that the crystallite size decreases to 13 nm after 10 h milling and thereafter crystallite size gets saturated. SEM indicated almost spherical shaped morphology of the milled powder. DSC revealed that as-received BaTiO$_3$ powder showed an endothermic peak at ~ 125°C which corresponds to Curie temperature of BaTiO$_3$. This Curie temperature was disappeared for the milled powder indicating transformation of tetragonal phase to cubic phase transition.

Introduction

With the ongoing trend of miniaturization of electronics, nanocrystalline ferroelectric ceramics are gaining importance for applications in capacitors, piezoelectric transducers, actuators, thermistors etc. [1-3]. Being a ferroelectric material, BaTiO$_3$ is a good candidate for such applications and its dielectric constant can be tailored depending upon its grain size, method of synthesis and purity [3,4]. It has been observed that the room temperature dielectric constant of coarse grained BaTiO$_3$ ($\geq$10 μm) increases with decreasing grain size and reaches a maximum at a grain size of ~1 μm. With further decrease in grain size, the dielectric constant decreases [5,6]. It has also been noted that below a certain critical size (~ 20 nm to 50 nm), ferroelectricity of BaTiO$_3$ particles disappears due to transformation from tetragonal to cubic phase [1,7]. Moreover, a peak corresponding to the Curie temperature of ferroelectric ceramic shifts to lower temperatures with decreasing particle size and below a critical size it may be disappeared [8]. Nanosized BaTiO$_3$ powders have been synthesized by a number of ways such as wet chemical method [5,9,10], sol-gel method [6], mechanochemical [11] and thermal decomposition method [7]. High energy ball milling has also been successfully used for the synthesis of nanopowders of PbZr$_{1-x}$Ti$_x$O$_3$, Sr$_{0.8}$Bi$_{2.2}$Ta$_2$O$_9$ [2,3], zinc oxide [12], iron [13], silicon carbide [14], Nd$_2$Fe$_{14}$B/Sm$_2$Co$_{17}$ [15], LiNbO$_3$ [16], ZrO$_2$ [17], Fe [18] etc. This technique is known to be simple, cost-effective and suitable for large scale production of nanopowders. Moreover, nanomaterials are attracting attention of researchers because of their excellent thermal, mechanical, electrical and optical properties [10,19-23]. Owing to high specific surface area nanoparticles provide good interface with the polymer matrices such as polystyrene [24], polymethylmethacrylate [4], polyvinylidene fluoride [25] and epoxy [8].

However, to the best of our knowledge, Curie temperature of the different sized BaTiO$_3$ nanoparticles which were synthesized by the high energy ball mill has not been reported, yet. In view of this, this paper focuses on the synthesis of nanocrystalline BaTiO$_3$ powder using a planetary ball mill in dry condition followed by characterization of the synthesized powders for morphology, crystallite/particle size and Curie temperature.

Experimental

Materials

Tetragonal BaTiO$_3$ powder was purchased from Sigma-Aldrich Co. Its reported particle size and density are < 2.0 μm and 6.08 g/cc, respectively.

Ball Milling

Ball milling of the BaTiO$_3$ powder was carried out in a planetary ball mill (PM 200, Retsch) using vials and balls made of zirconia in dry condition. The balls to powder ratio was maintained at 10:1. The rotational speed was set at 300 rpm [2] and the time for milling was varied from 5 h to 20 h in steps of 5 h.

Characterization of Ball Milled BaTiO$_3$ powders

BaTiO$_3$ powders ball milled for 5 h to 20 h were analysed by X-ray diffractometer (XRD, Philips X'Pert PANalytical PW 3040/60) using monochromatic CuK$_\alpha$ radiation over a 2θ angle from 10° to 90°. Crystallite size was determined from the peak broadening using the Scherrer equation (1) after taking instrumental error into consideration.

$$d = \frac{0.9\lambda}{\beta_c \cos\theta} \qquad (1)$$

$$\beta_c = \sqrt{\beta_n^2 - \beta_m^2}$$

Corresponding author. Tel.: 020-25507275; Fax: 020-25507299
E-mail address: rkgoyal72@yahoo.co.in

Where, β_c is corrected peak broadening (in radian) from nanopowder, β_n the peak broadening due to nanosized powder and β_m the peak broadening from the bulk $BaTiO_3$ powder. The λ is the wavelength of X-ray and θ is the Bragg angle.

The morphology and size of $BaTiO_3$ powders were studied using field emission scanning electron microscope (SEM, Zeiss, ∑igma). Particle sizes were also estimated from the Brunauer-Emmett-Teller (Smart Sob, India) method by finding the specific surface area (S.A.) using nitrogen as the adsorption gas. The particle size was calculated using equation (2).

$$d = \frac{6}{(S.A.).\rho} \qquad (2)$$

Where, ρ is the density of the $BaTiO_3$ powder. Modulated differential scanning calorimetry (MDSC Q20, TA Instruments, USA) was used to determine the Curie temperature of as received and ball milled powders. About 4-6 mg sample was sealed in an aluminium pan and heated from 30 ℃ to 200 ℃ at a heating rate of 5 ℃/min under nitrogen atmosphere. The data were recorded during first and second heating cycles to confirm the presence of stresses in the milled powders.

Results and Discussion

The XRD patterns obtained for powders milled for different time periods are shown in Figure 1, which show diffraction peaks at 2θ = 22.2°, 31.6°, 38.9°, 45.3°, 50.9°, 56.2° and 65.9° corresponding to the planes of (100), (110), (111), (200), (210), (211) and (220), respectively. This indicates that the $BaTiO_3$ powder has a pervoskite structure according to X'Pert High Score Plus file reference code 98-006-8257. The XRD patterns of the powder milled for 10 h and 20 h show significant peak broadening and less intense peaks as compared to the XRD pattern of the as received sample. The grain/crystallite size of various powders was determined from the Scherrer equation (1). It was found that the crystallite size decreased from 21 nm to 13 nm when the milling time increased from 5 h to 10 h. However, on further increasing the milling time to 20 h, the crystallite size remains 13 nm.
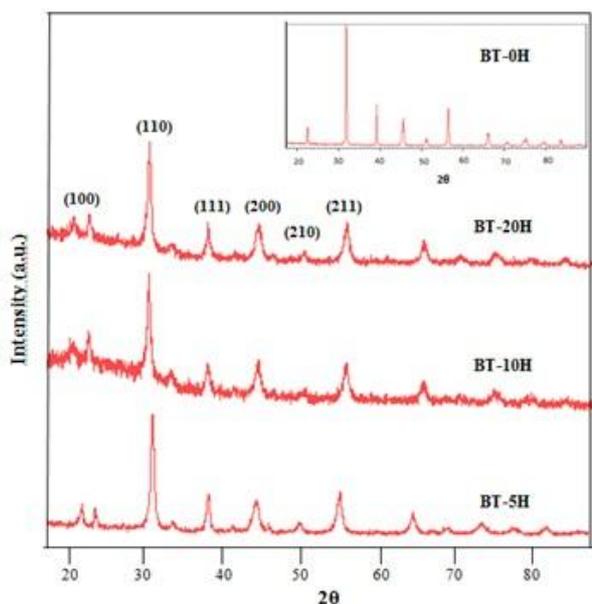
Figure 1: XRD patterns of BaTiO₃ powder after milling of 5 h (BT-5H), 10 h (BT-10H) and 20 h (BT-20H). Inset shows the XRD pattern of as received (0 h) BaTiO₃ powder.
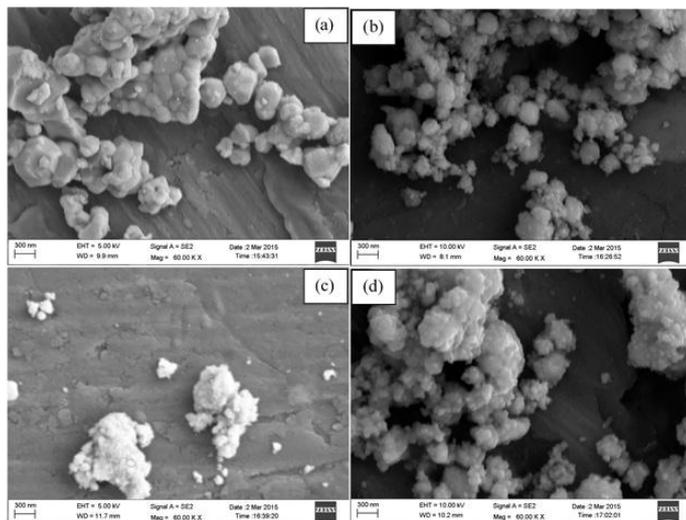
Figure 2: SEM images of BaTiO₃ powder after milling of (a) 0 h, (b) 5 h, (c) 10 h and (d) 20 h.

Figures 2a-d show SEM images of $BaTiO_3$ powder obtained after ball milling time of 0, 5 h, 10 h, and 20 h, respectively. As shown in Figure 2a, as received $BaTiO_3$ powder shows larger size secondary particles with size of more than 1.0 μm which consist primary particle (or crystallite) size of more than 100 nm. Figures 2b-d clearly show a reduction in $BaTiO_3$ powder size with increasing milling time. As shown in Figure 2b and 2c, after 5 hand 10 h, the particles size was reduced to a size of smaller than 100 nm. However, no significant difference in size was observed between the powders obtained after 10 h and 20 h of ball milling. The reason for the saturation in crystallite size or increase in particle size after a certain milling time particularly for the ceramics was not explained in literature. In contrast, aggregates of reduced particles/crystallites were formed due to the high surface energy associated with smaller crystallites. Brunauer-Emmett-Teller (BET) results indicated that the specific surface area increased with increasing milling time. Particle size calculated from equation (2) decreased from 45 nm to 27 nm and 23 nm when milling time increased from 5 h to 10 h and 20 h, respectively. The values of crystallites/particles size obtained from XRD and BET are tabulated in Table 1. There is some discrepancy between the sizes determined by XRD and BET. It is due to the fact that BET analysis measures particle size whereas XRD measures crystallite size (i.e., primary particle size or single crystal). It is also well known that the particles may be made up of a number of crystallites.

Table 1: Variation of particle/crystallite size with milling time

Ball milling time of BaTiO₃	Crystallite size (in nm) obtained from XRD	Particle size (in nm) from BET
5 h	21	45
10 h	13	27
20 h	13	23

Figure 3 shows the DSC scans of synthesized $BaTiO_3$ nanopowders. Each sample was subjected to two heating and cooling cycles. As received powder showed an endothermic peak at ~ 125°C (Curie temperature) corresponding to the tetragonal to cubic phase transition of $BaTiO_3$. As shown in Figure 3a, this peak was clearly seen in both the heating cycles. For 10 h milled powder, a peak was observed at about 95 °C during the first heating cycle but this peak was disappeared during the second heating cycle (Figure 3b). The peak observed in the first cycle may

probably be attributed because of strains (or stresses) induced during the milling process which are released after absorbing thermal energy during first heating cycle. Similar behaviour with more intensity was observed for the 20 h milled powder, as shown in Figure 3c. Disappearance of the peak corresponding to Curie temperature signifies that tetragonal to cubic transition has already taken place in the $BaTiO_3$ due to reduction in particle size [7].
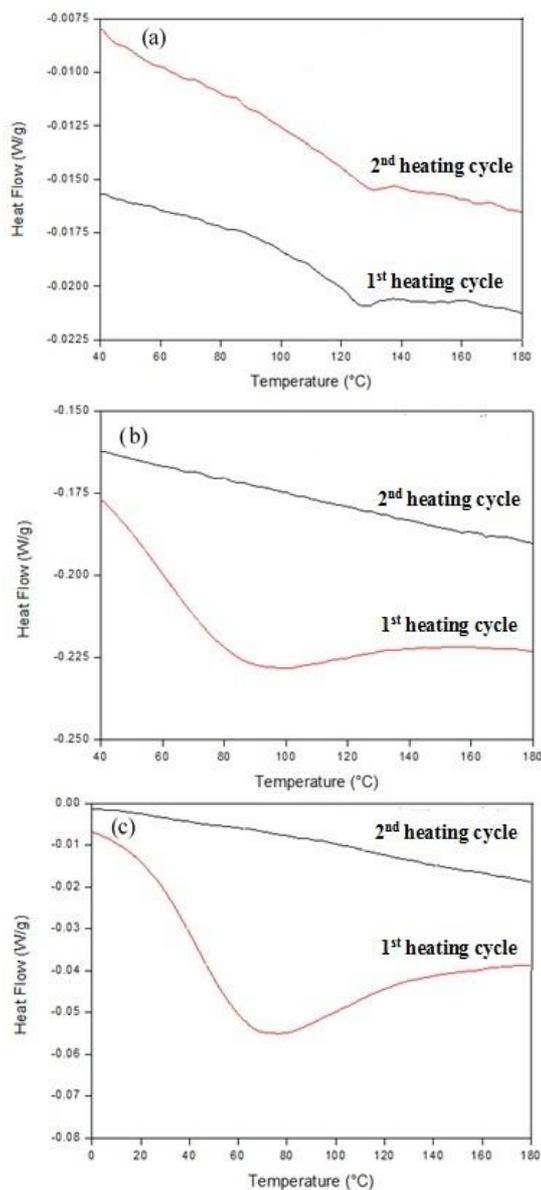
Figure 3: DSC heating and cooling scans of $BaTiO_3$ powder after milling of (a) 0 h, (b) 10 h and (c) 20 h.

Conclusions

$BaTiO_3$ nanopowders was successfully synthesized using a planetary ball mill in dry condition at ball to powder ratio of 10:1 and speed of 300 rpm. The lowest crystallite size obtained was 13 nm after 10 h and on further milling there was no decrease in crystallite size. SEM indicated almost spherical shaped morphology of the milled powder. DSC showed that the milled nanopowders gradually transformed from tetragonal to cubic phase as milling time increased and the Curie temperatures of the milled nanopowders disappear.

References

1. Suryanarayana, C.; Progress in Materials Science 46 (2001) 1-184.
2. Nath, A.K.; Singh, J.K.; Physica B. 2010, 405, 430–434.
3. Sugandha; Jha, A.K.; Materials Characterization 2012, 65, 126 – 132.
4. Goyal, R.K.; Katkade, S.S.; Mule, D.M.; Composites: Part B 2013, 44, 128 – 132.
5. Park, J.H.; Yoo, D.H.; Kim, C.S.; Yang, H.S.; Moon, B.K.; Jung, G.J.; Jeong, E.D.; Hong, K.S.; Journal of the Korean Physical Society 2006, 49, 680 – 683.
6. Luan, W.; Gao, L.; Guo, J.; Ceramics International 1999, 25. 727 – 729.
7. Wada, S.; Hoshina, T.; Yasuno, H.; Nam, S.M.; Kakemoto, H.; Tsurumi, T.; Yashima, M.; Journal of the Korean Physical Society 2005, 46 (1), 303 -307.
8. Yang, W.; Yu, S.; Luo, S.; Sun, R.; Liao, W.; Wong, C.; Journal of Alloys and Compounds 2015, 620, 315-323.
9. Wang, X.; Chen, R.; Gui, Z.; Li, L.; Materials Science and Engineering B 2003, 99, 199 – 202.
10. Kobayashi, Y.; Tanase, T.; Tabata, T.; Miwa, T.; Konno, M.; Journal of the European Ceramic Society 2008, 28, 117 – 122.
11. B.D. Stojanovic, A.Z. Simoes, C.O. Paiva-Santos, C. Jovalekic, V.V. Mitic, J.A. Varela. J. Eur. Cer. Soc. 25 (2005) 1985–1989.
12. Amirkhanloun, S.T.; Ketabchi, M.P.; Parvin, N.D.; Materials Letters 2012, 86, 122 – 124.
13. Goyal, R.K.; Dhoka, P.; Bora, A.; Gaikwad, P.; Journal of Materials Science & Surface Engineering (JMSSE), 2016, 4(1), 339-341.
14. Rao, J.P.; Kush, D.H.; Bhargava, N.M.; Journal of Minerals & Materials Characterization & Engineering 2012 11, 529 - 541.
15. Indris, S.S.; Bork, D.; Heitjans, P.; Journal of Materials Synthesis and Processing 2000, 8(3), 245 - 250.
16. Poudyal, N.; Altuncevahir, B.; Chakka, V.; Chen, K.; Black, T.D.; Liu, J.P.; Ding, Y.; Wang, Z.L.; J Phys. D: Appl. Phys. 2004, 37, L45 - L48.
17. Goyal R. K., Deshpande S.P., Singare S.S. Journal of Materials Science & Surface Engineering, 2016, 4 (2), 360-363.
18. Goyal R. K., Dhoka P., Bora A., Gaikwad P. Journal of Materials Science & Surface Engineering, 2016, 4 (1), 339-341.
19. Olmos, D.; Martinez-Tarifa, J.M.; Gonzalez-Gaitano, G.; Gonzalez-Benito, J.; Polymer Testing 2012, 31, 1121 – 1130.
20. Sebastian, M.T.; Jantunen, H.; Int. J. Appl. Ceram. Tech. 2010, 7 [4] 415 – 434.
21. Wankhede Y. B., Kondawar S. B., Thakare S. R., More P. S. Adv. Mat. Lett. 2013, 4(1), 89-93.
22. Bandyopadhyay M., Hermann Gies, Grünert W., Berg M.V. D., Birkner A. Adv. Mater. Lett. 2015, 6(11), 978-983.
23. Kulkarni M., Mazare A., Schmuki P., Iglic A. Adv. Mater. Lett. 2016, 7(1), 23-28.
24. Goyal, R.K.; Tiwari, A.N.; Mulik, U.P.; Negi, Y.S.; J. Phys. D: Appl. Phys. 2008, 41, 85403.
25. Mendes, S.F.; Costa, C.M.; Caparros, C.; Sencadas, V.; Lanceros-Mendez, S.; J. Mat. Sci. 2010, 47, 1378 – 1388.